PROPAGATION SPEED IN MYELINATED NERVE

II. THEORETICAL DEPENDENCE ON EXTERNAL Na^+ AND ON TEMPERATURE

W. L. HARDY

From the Department of Physiology and Biophysics, University of Washington School of Medicine, Seattle, Washington 98195. Dr. Hardy's present address is the Department of Physiology, Boston University School of Medicine, Boston, Massachusetts 02118.

ABSTRACT The Hodgkin-Huxley (H.H.) equations modified by Dodge for *Rana pipiens* myelinated nerve have been solved to determine how well the theory predicts the effects of changes of temperature and $[Na^+]_0$ on propagation. Conduction speed θ was found to have an approximately exponential dependence on temperature as was found experimentally, but the theoretical temperature coefficient (Q_{10}) was low; 1.5 compared with the experimental finding of 2.95. θ was found to be a linear function of log ($[Na^+]_0$) in contrast to the experimental finding of a square root dependence on $[Na^+]_0$. θ is 50% greater at one-fourth normal $[Na^+]_0$ than the theory predicts. The difference between the theoretical $\theta([Na^+]_0)$ and the experimental $\theta([Na^+]_0)$ is probably due to an imprecisely known variation of parameters and not to a fundamental inadequacy of the theory.

INTRODUCTION

An experimental study (Hardy, 1973) has shown that conduction speed (θ) in single axons of *R. pipiens* myelinated nerve is a power function of $[Na^+]_0$ and that the power is very close to 0.5; i.e., that $\theta_1/\theta_2 = SQRT([Na^+]_1/[Na^+]_2)$. This paper presents the results of a theoretical analysis of impulse propagation in *R. pipiens* myelinated axons for conditions similar to the physical conditions of the experiments. The principal purpose of this study is to determine how closely the H.H. theory applied to a myelinated axon predicts the experimental findings and to attempt to identify the reasons for the differences.

The effects of variations of most of the passive electrical parameters and some of the geometrical parameters on conduction speed in *R. pipiens* myelinated nerve fibers have also been determined and will be published in a separate paper.

Various experimental results have previously been compared with predictions based on solutions of the H.H. (1952) equations for myelinated nerve fibers using

both the original H.H. equations for squid and the equations and numerical parameters of Frankenhaeuser and Huxley (1964) for *Xenopus laevis*.

FitzHugh (1962) used the H.H. equations and data for squid to investigate impulse initiation and saltatory conduction in myelinated fibers. Then Goldman and Albus (1968) used the numerical parameters for *X. laevis* in a study of the theoretical basis of the speed-diameter relationship. Subsequently Smith and his co-workers investigated the relationship between speed and temperature (Hutchinson et al., 1970) and between speed and myelin thickness (Smith and Koles, 1970).

The equations have been derived and numerical constants evaluated for propagation in large myelinated nerves of *R. pipiens* (Dodge, 1961, 1963; see also Hille, 1971 *b*). Although equations for this preparation have not previously been solved for propagated responses, theoretical calculations using them have been compared with results from experiments on voltage-clamped nodes (Bennett et al., 1970; Hille, 1970). (Preliminary reports on studies of propagation have been published [Hardy and Woodbury, 1970; Hardy, 1971].)

The full set of equations and the numerical parameters for a large *R. pipiens* myelinated nerve worked out by Dodge (1963) ("node 7") and slightly modified by Hille (1967) have been published by Hille (1971 *a*). Hille (1970) has also compared the equations for mathematical models of nodes of Ranvier of large *X. laevis* and *R. pipiens* myelinated axons with the equations for squid (*Loligo*) giant axons.

METHODS

Equations and Constants

The model system employed is similar to that of FitzHugh (1962). The complete basic set of equations follows (symbol definitions and the numerical values of parameters are given in Table I).

Internode. The transmembrane potential $E_M(x, t)$ is assumed to satisfy the cable equation in the internodal region:

$$c_m \frac{\partial E_M(x,t)}{\partial t} = \frac{1}{r_i + r_0} \frac{\partial^2 E_M}{\partial x^2} - \frac{(E_M - E_r)}{r_m}. \qquad (1\,a)$$

To facilitate numerical solution, Eq. 1 *a* was converted in the usual way to a difference-differential equation for short segments of internode (see Numerical Methods). For the calculations reported in this paper, nodes were spaced 2 mm apart. For computation, internodes were divided into five segments. This makes the distance between points of calculation less than $\frac{1}{10}$ the space constant of the internode.

For each discrete segment k of internode,

$$\frac{dE_k}{dt} = \frac{1}{c_m(r_i + r_0)(\Delta l)^2}[E_{k+1} + E_{k-1} - 2E_k] - \frac{(E_k - E_r)}{r_m c_m}, \qquad (1\,b)$$

where Δl is the length of a segment of internode and E_{k-1} and E_{k+1} are the membrane potentials across the lumped segments on either side of segment k.

TABLE I

SYMBOL DEFINITIONS AND NUMERICAL VALUES OF PARAMETERS

Parameter	Definition and units	Value of parameter at 22°C	
		Standard data set (SDS)	Computational data set (CDS) if different from the SDS
θ	conduction speed (m/s)	—	—
D	fiber diameter (μm)	14	—
δ	myelin thickness (μm)	2	—
l	internodal spacing (cm)	0.2	—
A	area of nodal membrane (μm)^2	22	—
r_i	resistance/unit length of axis cylinder (MΩ/cm)	150*	140*
r_0	resistance/unit length of extracellular space (MΩ/cm)	negligible	—
r_m	resistance $\times$ unit length of myelin sheath (MΩ-cm)	29*	40*
c_m	capacity/unit length of myelin sheath (pF/cm)	16	10
C_N	capacity of node (pF)	2	0.6
$E_M(x, t)$	membrane potential in internodal region [potential inside—outside] (mV)	—	—
$E_N(t)$	membrane potential at node (mV)	—	—
$I_N(t)$	total current flowing outward through nodal membrane (nA)	—	—
E_r	resting membrane potential (mV)	−75	variable†
E_L , E_K	equilibrium potential for "leakage" ions and K^+ (mV)	−75	variable†
E_{Na}	equilibrium potential for Na^+ (mV)	48*	variable§
$[Na]_i$	intracellular Na^+ concentration (mM/liter)	16.664	—
$[Na]_0$	extracellular Na^+ concentration (mM/liter)	110	27.5–137.5
g_L	"leakage" conductance of node ($\mu\Omega$)	0.025*	0.0125*
$\bar{g}_K$	K^+ conductance of node ($\mu\Omega$)	0.13	—
$\bar{P}_{Na}$	Na^+ permeability constant for node (cm^3/s)	3.9×10^{-9}*	5×10^{-9}*
m, h	Variables for activation and inactivation of P_{Na} (dimensionless)	$m(E, t)$	—
		$h(E, t)$	—
n	Variable for activation of g_K (dimensionless)	$n(E, t)$	—
α, β	rate constants for temporal variations of m, h, and n (ms^{-1})	$\alpha(E)$*	—
		$\beta(E)$*	—
R	gas constant (J/deg-mol)	8.3144	—
F	faraday (C/g-eq)	96,487	—
T	absolute temperature (°K)	273.16	variable
Δt	numerical integration (time) interval (μs)	0.2–0.8	—

References: parameters D through c_m after Hodgkin, 1964 (most are from Huxley and Stämpfli, 1951 *a* and *b*, and Tasaki, 1955); parameters E_r through P_{Na} and equations for rate constants after Dodge (1961, 1963) and Hille (1967).

* Varied with temperature (see text).

† Increased by −2 mV for each 50% decrease in $[Na^+]_0$ (Huxley and Stämpfli, 1951 *a*).

§ Varied with $[Na]_0$ and T (Nerst equation).

Node. The nodal membrane is assumed to be isopotential (Dodge, 1963) and the potential to satisfy the equation

$$C_N(\mathrm{d}E_N/\mathrm{d}t) = I_N - g_L(E_N - E_L) - g_K n^4(E_N - E_K) - \bar{P}_{Na} m^3 h \mathcal{G}_{Na}, \quad (2)$$

where

$$\mathcal{G}_{Na} = E_N \psi \left(\frac{[Na]_0 - [Na]_i \exp \psi}{1 - \exp \psi} \right), \qquad \psi = \frac{E_N F}{RT}. \quad (3)$$

Each of m, h, and n is assumed to obey an equation of the form

$$\mathrm{d}s/\mathrm{d}t = \alpha_s(1 - s) - \beta_s s, \qquad s = m, h, n, \quad (4)$$

with forward (α) and backward (β) rate constants given by

$$\alpha_m = \frac{-1.6\, a}{\exp(-a) - 1} + \Delta\alpha, \qquad a = \frac{E_N + 37.5}{3.8}, \quad (5)$$

$$\Delta\alpha = \frac{6}{1 + b^2}, \qquad b = \frac{E_N + 25}{18}, \quad (6)$$

$$\beta_m = \frac{4.05\, c}{\exp(c) - 1}, \qquad c = \frac{E_N + 37.5}{13.2}, \quad (7)$$

$$\alpha_h = \frac{0.14\, d}{\exp(0.8\, d) - 1}, \qquad d = \frac{E_N + 79}{5.9}, \quad (8)$$

$$\beta_h = \frac{4.0}{\exp(-e) - 1}, \qquad e = \frac{E_N + 17}{14.5}, \quad (9)$$

$$\alpha_n = \frac{-0.34\, f}{\exp(-f) - 1} + 0.1, \qquad f = \frac{E_N + 15}{15.9}, \quad (10)$$

$$\beta_n = \frac{0.085\, g}{\exp(g) - 1}, \qquad g = \frac{E_N + 37.5}{12.2}, \quad (11)$$

(Dodge, 1963, "node 7" slightly modified by Hille, 1967).

Continuity and Boundary Conditions. The potential difference E between axoplasm and external solution must be a continuous function of the axial distance variable x. (As noted in the above section $E_N(t)$ is assumed independent of x within the nodal axoplasm.) Therefore the potential across the myelin sheath must approach the potential across the nodal membrane at the node-internode junction. At the center of node q, $x = ql$ where l is the internodal spacing, assumed invariant. At the boundary between node q and the internode on both sides,

$$\lim_{\Delta x \to 0} E_M(ql \pm [\Delta x + w], t) = E_N(t), \quad (12)$$

where w is the width of the nodal cylinder (also invariant). Since $w \ll l$, w may generally be neglected when converting conduction times to conduction speeds.

The total current flowing out through the membrane of node q is the difference between the axial current entering the axoplasm of the nodal cylinder from the internode on one end and the current leaving the cylinder at the other end. Thus

$$I_N = \frac{1}{r_i + r_0}\left\{\lim_{\Delta x \to 0} \frac{\partial E_M (ql - [w + \Delta x], t)}{\partial x} - \lim_{\Delta x \to 0} \frac{\partial E_M (ql + [w + \Delta x], t)}{\partial x}\right\}, \quad (13\,a)$$

where current flowing in the positive x direction in the axoplasm is taken as positive current. The computational form of Eq. 13 *a* is

$$I_N = \frac{1}{(r_i + r_0)\Delta l}\{(E_{q+\Delta l} - E_q) - (E_q - E_{q-\Delta l})\}, \quad (13\,b)$$

where $E_{q+\Delta l}$ and $E_{q-\Delta l}$ are the potentials across the myelinated internode on adjacent segments at each side of node q. The leakage and capacity of a half segment of internode on either side of a node are included in the leakage and capacity of the node.

At the stimulated node, $(q = 0)$, by symmetry:

$$I_{N_0} = \left\{\lim_{\Delta x \to 0} \frac{\partial E_M}{\partial x}(w + \Delta x, t)\right\} \frac{2}{r_i + r_0} + I_s, \quad (14\,a)$$

where I_s is the stimulus current, a square wave lasting 100 μs and of sufficient strength to elicit an action potential (AP) for all trials of a given set of calculations. The computational form of Eq. 14 *a* is

$$I_{N_0} = \frac{2}{(r_i + r_0)\Delta l}(E_{0+\Delta l} - E_0) + I_S. \quad (14\,b)$$

At the terminal internode, $r_m \to 0$. This is operationalized by making the membrane potential across the internodal membrane beyond the last node exactly equal to the potential at the last node. This artifice simplifies the computations and permits a relatively short segment of nerve to be a quite satisfactory model. It results in an apparent increase, by less than 2 mV, in the height of APs at the terminal node compared with the height at more central nodes.

Goldman and Albus (1968) chose to short-circuit the terminal node in their model system. This results in at least a 6 mV perturbation of the membrane potential at a distance of one node from the end (Hutchinson et al., 1970, Fig. 3), and thus the perturbation at the terminal node is considerably greater than that which results from the boundary condition I used. For normal conditions (normal internodal space constant and normal $[Na^+_0]$) no visually detectable perturbation of the AP can be seen at a distance greater than two nodes from the nerve end. With a decrease in $[Na^+]_0$, the perturbation in the terminal node membrane potential is increased to 5 mV for $[Na^+]_0$ = 27.5 mM/liter) and the perturbation can then be detected 3 but not 4 nodes from the end.

Temperature Dependence of Parameters. Dodge evaluated g_L, $\bar{g}_K$, $\bar{p}_{Na}$ and the rate constants for *R. pipiens* myelinated nerve nodes at 22°C. Most of the other node and internode parameters have been evaluated at room temperature (24–25°C, Tasaki, 1955; 17°C, Huxley and Stämpfli, 1951 *a*). Since the experiments on the effects of $[Na^+]_0$ on θ were undertaken at 15°C (Hardy, 1973), the numerical parameters used have been corrected to 15°C. No temperature corrections were made for the capacities c_m and C_N although Taylor and Chandler (1962) have reported a slight increase (1% per degree centigrade) in

the capacity of the squid giant axon membrane with increase in temperature. Leakage currents through the myelin and the nodal membrane, and current flowing along the axoplasm have been assumed to behave like ion currents in simple electrolytes and a Q_{10} of 1.2 has been used for the corresponding conductances. Other temperature coefficients for *R. pipiens* have been assumed to be similar to those obtained by Frankenhaeuser and Moore (1963) for large myelinated fibers of *X. laevis*.

Numerical Methods

The set of equations (Eqs. 3–15) was solved numerically using a digital analogue-computer simulation program (DAS).[1] A modified Euler method of numerical integration was used in solving the equations (Kelley, 1967). The integration interval Δt was not varied during a given simulation but was adjusted between runs when necessary to assure stability and accuracy.

Solution of the set of equations for an isolated single node ($I_N = 0$ in Eq. 2) using the standard data set (SDS) of Table I and $\Delta t = 1$ μs gave excellent agreement with the original experimental AP (Dodge, 1963, node 7) and with a numerical solution by Hille using a Fortran program (personal communication). Graphs of the two theoretical results almost exactly superimposed. The solution of $E_N(t)$ for a 4 μs segment of real time requires 20 s of computation time. From an analysis of the effects of varying Δt, I found no instability in the solution for a single node for a wide range of integration intervals ($0.01 \leq \Delta t \leq 8$ μs) and plots of $E_N(t)$ from these solutions were found to superimpose over most of their time-courses. The maximum value of dE_N/dt was compared for $\Delta t = 8$, 1 and 0.01 μs. Taking the value with $\Delta t = 0.01$ μs as the standard, the maximum value of the derivative was less than 0.4% lower at $\Delta t = 1$ μs and 3% lower with $\Delta t = 8$ μs.

The addition of the cable equation to the computation was found to introduce instabilities unless Δx and Δt were suitably chosen (previously reported by Goldman and Albus, 1968). A stable solution was generally obtained using $\Delta t = 1$ μs. Most computations reported here were made with a Δt of 0.2–0.4 μs. For $\Delta t = 0.4$ μs, about 10 min of computational time was required per millisecond of simulated time. Included in the computations was the collection and storage in memory of the time-courses of up to 30 variables.

Conduction speed was calculated directly by the computer from the difference in time of occurrence of the maximum rate of rise of the AP at nodes 4 and 5. As a check on this calculation, the difference in time of occurrence of the peak of the AP at nodes 4 and 5 was also detected. The two results were usually identical, but occasionally they differed by a small (1–3) integral multiple of the integration interval. Conduction speed was found to be independent of the nodes chosen for the calculations, provided the nodes were not closer than 2 or 3 from the ends of the simulated nerve.

RESULTS

The Propagated Response

The initial results from calculations provided an unexpected finding (Fig. 1 *a*). Conduction speed (9.5 m/s) was approximately half of the expected value and even

[1]The computations were made on a Raytheon PB 440 digital computer (8k, 24-bit main memory with 3 μs cycle time and a stored-Logic biax memory of 512 words with 200 ns nondestructive readout time). Computations were made using a 39 bit floating-point fraction and an 8 bit exponent. Input and output numerical parameters have 9 and 5 significant digits, respectively.

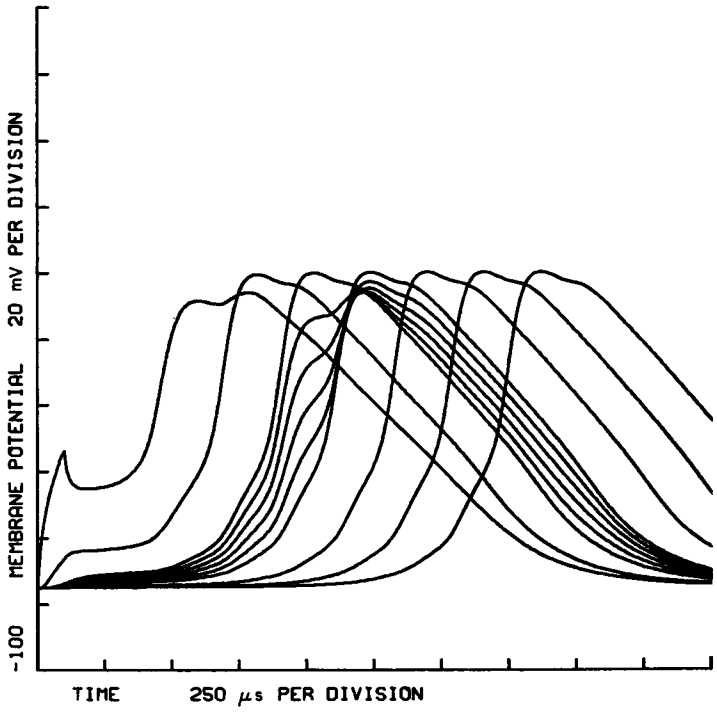

FIGURE 1 *a* Membrane potential at nodes 0 through 7 and at 4 internodal locations between nodes 2 and 3 during propagation. RP = −75 mV, $[Na^+]_0$ = 110 mM/liter, temperature 15°C. "Standard Set" of numerical parameters (Table I).

more disturbing, the shape of the AP was clearly distorted as compared with the shape seen under experimental conditions. The shape of $E_N(t)$ at a given node was directly influenced by the AP at adjacent nodes; the occurrence of the peak of the AP at adjacent nodes could clearly be detected on the wave form.

Since the single node solution was satisfactory, errors were looked for in the solution of the cable equation and in the coupling between nodes and internodes. The tests included simulation of the conditions for measuring space and time constants, simulation of an injection of a fixed charge into node 0 (with g_L and $1/r_m$ set to zero) and simulation of a space-clamped AP. No abnormal results were found in any of the tests. The original finding of an abnormally slow conduction speed then was taken as an indication that the various resistances and capacities used might require modification. Conduction speed was computed for various numerical values of each of the passive numerical parameters. For the calculated AP shown in Fig. 1 *b*, conduction speed has been increased to 18.90 m/s and no evidence is seen of the original perturbation. However, when propagation is slowed (by lowering the temperature or decreasing $[Na^+]_0$) the perturbation again becomes visible (Fig. 4).

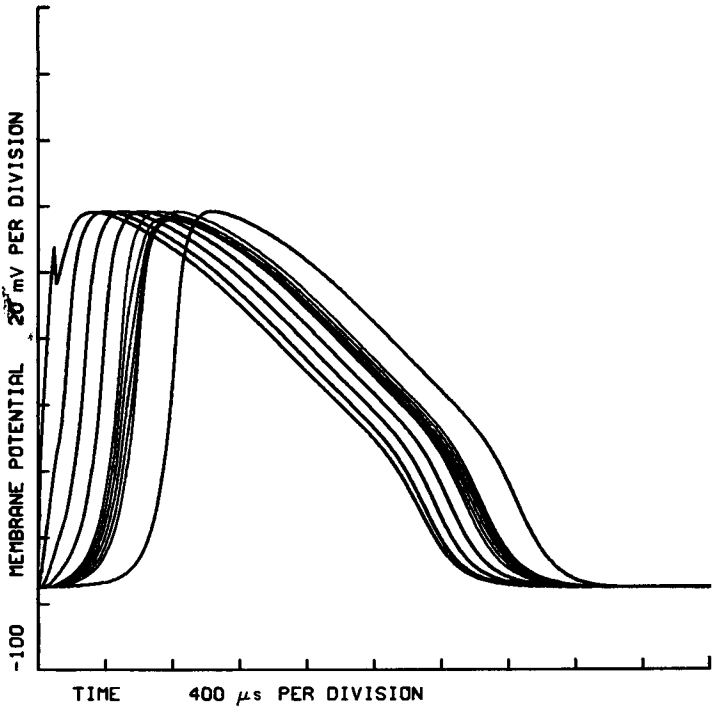

FIGURE 1 *b* Same physical conditions as in Fig. 1 *a* except the adjusted numerical parameters used (computational data set, Table I).

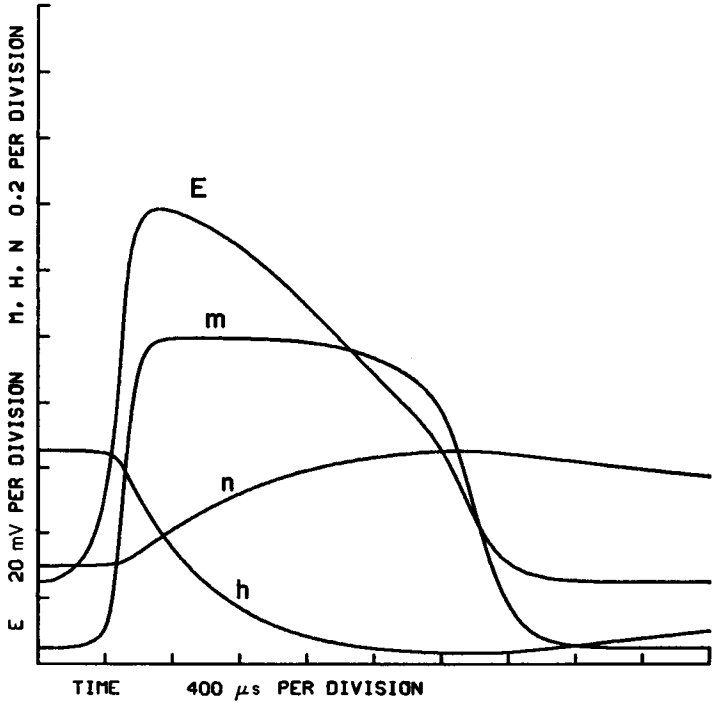

FIGURE 1 *c* Membrane potential and *m*, *h*, and *n* at node 4 during propagation. Same physical conditions as in Fig. 1 *b*.

The final values used for the numerical constants in this study are given in Table I, column 4. The adjusted values are all within the range of the experimentally observed values (Hodgkin, 1964, Table 4). An increase in $\bar{P}_{Na}$ from 3.9 to 5 $\times$ 10^{-9} cm^3/s was also an arbitrary adjustment to speed up propagation. Dodge (1963) has reported values for this parameter in voltage-clamped frog nodes ranging from 2.4 to 5.35 $\times$ 10^{-9} cm^3/s.

An extended effort was made to insure that this arbitrary adjustment of constants did not modify the basic conclusions to be drawn on the theoretical effects of temperature and $[Na^+]_0$ on θ. Conduction speeds in solutions of different $[Na^+]_0$ were computed for a range of each of the modified parameters. The slopes and intercepts of the plots of speed as a function of $[Na^+]_0$ varied by a few percent with the adjustment of the numerical parameters, but the general shape of the graphs was not significantly altered.

Currents Flowing during Propagation

Graphs of the nodal and internodal membrane currents and axial current during propagation are shown in Figs. 2 *a* and 2 *b*. The total ion current through the nodal membrane, the total current out through the myelin sheath, and the longitudinal

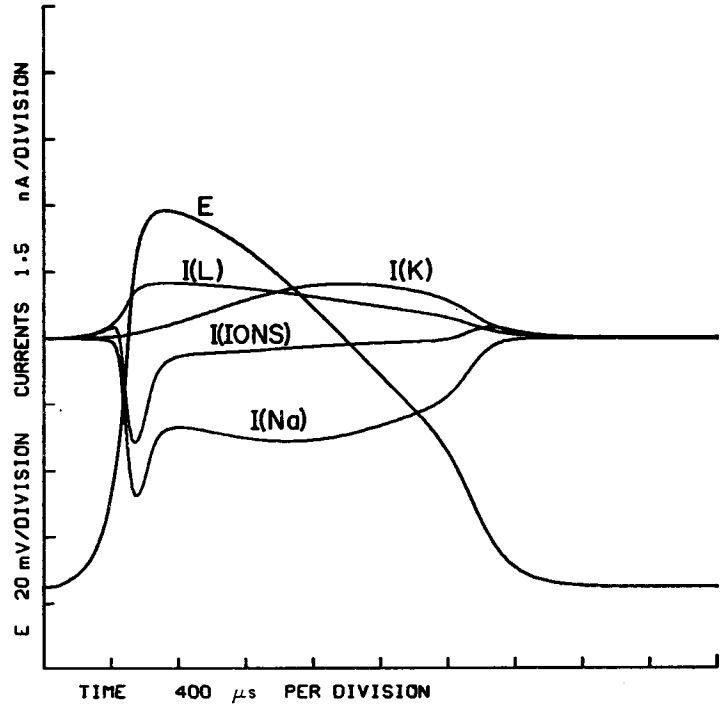

FIGURE 2 *a* Membrane potential and Na, K, leakage, and total ion currents through the membrane of node 4 during propagation. $[Na^+]_0$ = 110 mM/liter, temperature 15°C.

current flowing along the internode all are comparable in form with the available experimental data (Huxley and Stämpfli, 1949). The magnitude of the theoretical currents are perhaps slightly less (under 2 nA for the maximum longitudinal current compared with 2.5–3.5 nA from the experimental data) but the conduction speed is also less. The simulated axon may therefore correspond to a slightly smaller fiber than that observed by Huxley and Stämpfli. Also the simulation was for a lower temperature (15°C) compared with 18–20°C for Huxley and Stämpfli's experiments.

Effect of Temperature on Conduction

Fig. 3 shows the theoretical dependence of θ, $(dE_N/dt)_{max}$ and $(E_N)_{max}$ on temperature. In these simulations, none of the values, resting potential (RP), E_{Na} or E_k, were made to vary with temperature.

The effect of temperature on I_{Na} occurs through both $\bar{P}_{Na}$ and g_{Na}. The computations show that both θ and $(dE_N/dt)_{max}$ increase approximately exponentially

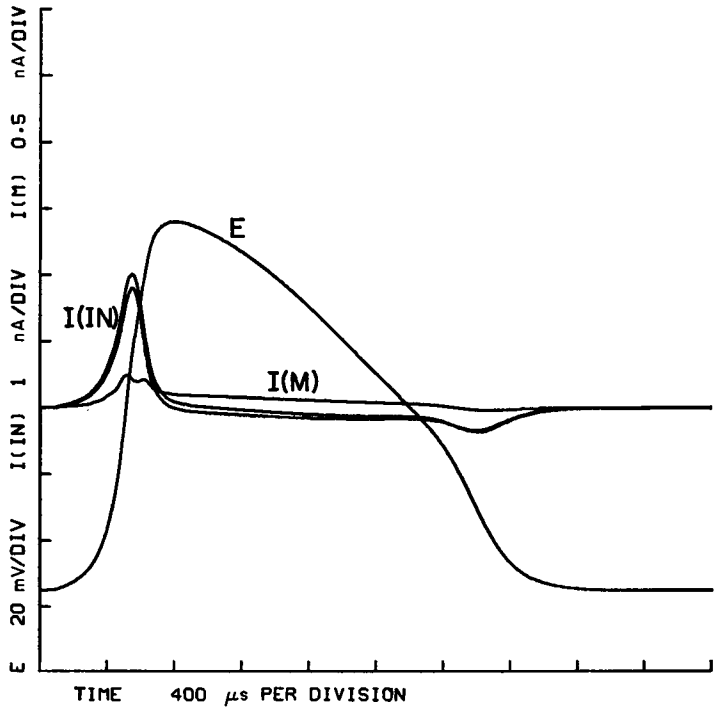

FIGURE 2 *b* Membrane potential and longitudinal and radial currents in the internodal region at a point 0.8 mm past node 4. The current flowing out through the myelin (radial current) at this point (curve with double hump) is shown at double the scale of the longitudinal currents flowing up to and away from the point. $[Na^+]_0$ = 110 mM/liter, temperature 15°C.

(Figs. 3 *a*, 3 *b*) as temperature is increased from 0 to 25°C (Q_{10}'s of 1.50 and 1.69, respectively). There is a gradual change in the slope of both curves as temperature is further increased, which indicates that neither of these variables had an exact exponential dependence on temperature. This result is in sharp contrast with a computer simulation study of propagation in myelinated nerves by Hutchinson et al. (1970). They found a linear dependence of θ on temperature. However, these authors did not include in their calculations the temperature dependence of all of the parameters known to vary with temperature (personal communication).

The height of the simulated AP does not vary monitonically with temperature; the plot shows a very broad maximum between 0 and 15°C, (Fig. 3 *c*) with the peak occurring at about 8°C. Above 25°C there is a very rapid decline in height as temperature is increased. The computations become increasingly more time consuming at temperatures above 40°C, since the maximum rate of rise of the AP is a full order of magnitude greater than at 0°C and a much finer integration interval is required to maintain accuracy.

Effect of Changes of $[Na^+]_0$ on Conduction

The effects of changes of $[Na^+]_0$ on the shape of the simulated propagated AP are shown in Fig. 4. Generally, the maximum values of the AP and of most currents decline as $[Na^+]_0$ is reduced. However, the maximum axial current flowing in the

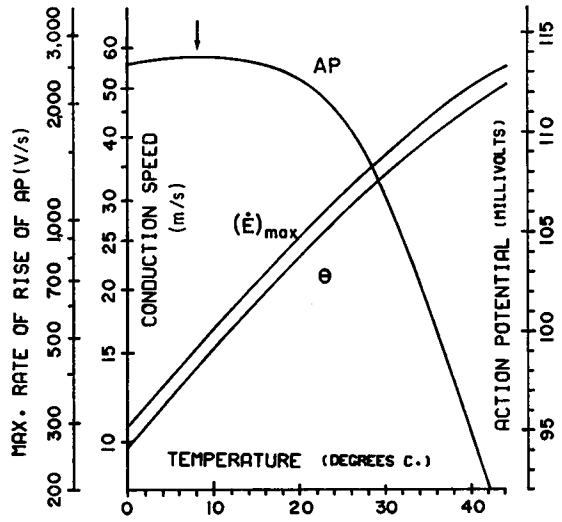

FIGURE 3 The theoretical effect of temperature on conduction speed (θ), on the maximum rate of rise $(\dot{E})_{max}$, and on the height of the AP in a myelinated nerve. The calculated Q_{10} of θ over the region 10–20°C. is 1.5 and for $(\dot{E})_{max}$ it is 1.7. The RP has been artificially held constant at −75 mV, whereas ion equilibrium potentials were varied with temperature. The arrow indicates the temperature of the maximum height of the AP occurring near 8°C.

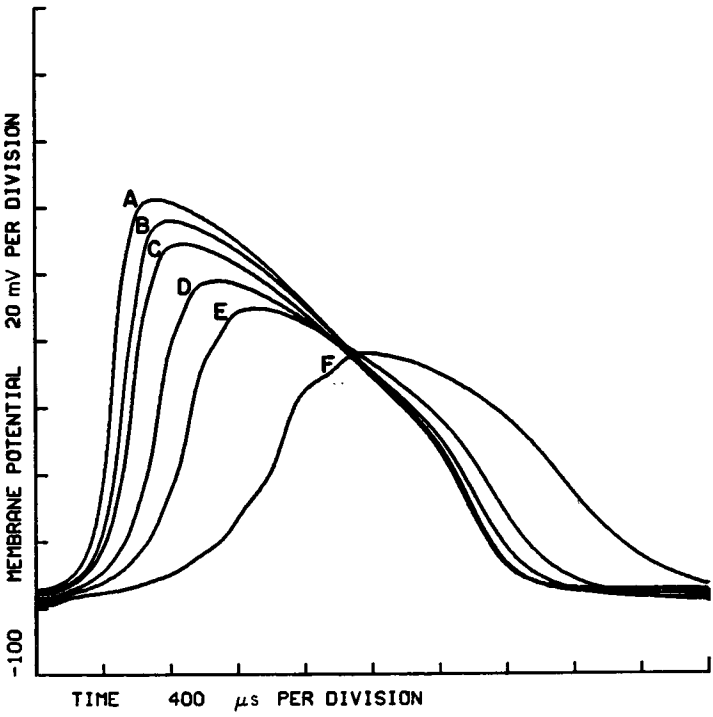

FIGURE 4 Changes in AP at node 5 during propagation resulting from changes in $[Na^+]_0$. Relative $[Na^+]_0$ are as follows: A, 137.5; B, 110; C, 82.5; D, 55; E 41.25; F, 27.5. Temperature 15°C.

internode during the repolarization phase becomes larger, increasing from 0.3 to 0.5 nA as $[Na^+]_0$ is reduced from 110 to 27.5 mM/liter. A reduction in $[Na^+]_0$ does result in a smaller axial current flowing during the depolarizing phase; the decline is by about one-half.

The theoretical effect of $[Na^+]_0$ on conduction speed is compared with the experimental results in Fig. 5. The experimental curve is drawn according to the equation $\theta = 18.90\ ([Na^+]_0/110)^{0.52}$ whereas the theoretical result is that speed increases very close to linearly with log $[Na^+]_0$. There is no real difference between the theoretical and experimental curves for $[Na^+]_0 > 70$ mM/liter. However, for the lower values of $[Na^+]_0$, the real nerve is able to conduct significantly faster than is predicted by the theory.

The variations of a number of calculated parameters are plotted in Fig. 6 as functions of log $[Na^+]_0$. The maximum rate of rise of the AP and conduction speed both vary nearly linearly with log $[Na^+]_0$. The peak of the AP and the maximum value of I_{Na} both increase monotonically but not linearly with log $[Na^+]_0$.

Hodgkin has suggested that θ should vary with the square root of the rate of rise of the AP (Hodgkin and Katz, 1949). This prediction can be tested using the calcu-

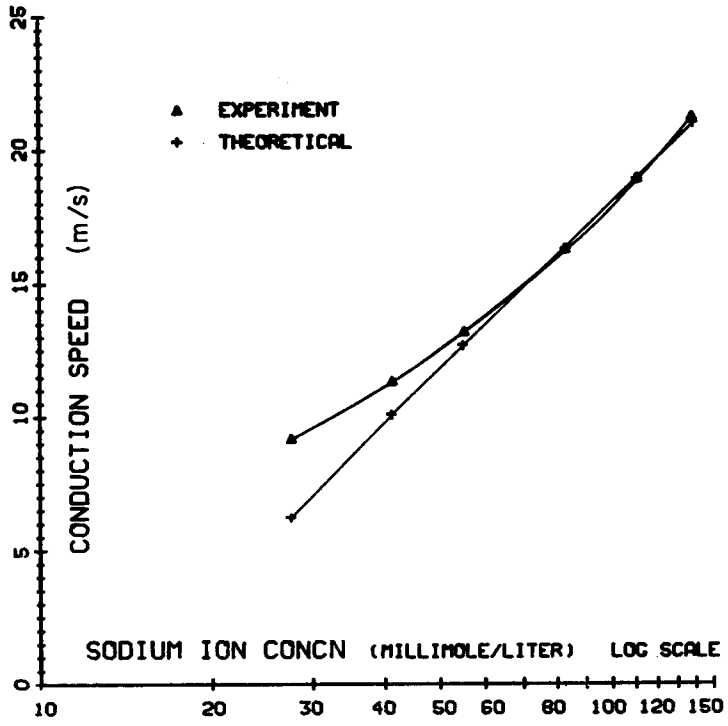

FIGURE 5 A comparison of the theoretical (+) and experimental (▲) dependence of conduction speed on $[Na^+]_0$ at 15°C. The experimental curve has been drawn according to the equation $\theta = 18.90([Na^+]_x/110)^{0.62}$.

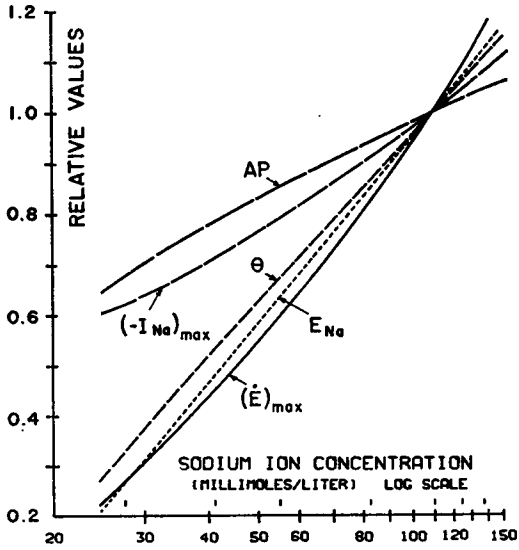

FIGURE 6 The theoretical effects of variations of $[Na^+]_0$ around the standard value of 110 mM/liter at 15°C. The absolute values of the parameters at $[Na^+]_0 = 110$ mM/liter are as follows: height of the AP (AP), 113.47 mV; max Na^+ current ($-I_{Na}$), 3.575 nA; conduction speed (θ), 18.904 m/s; sodium equilibrium potential (E_{Na}), 46.86 mV; maximum rate of rise of the AP $(\dot{E})_{max}$, 684.8 V/s.

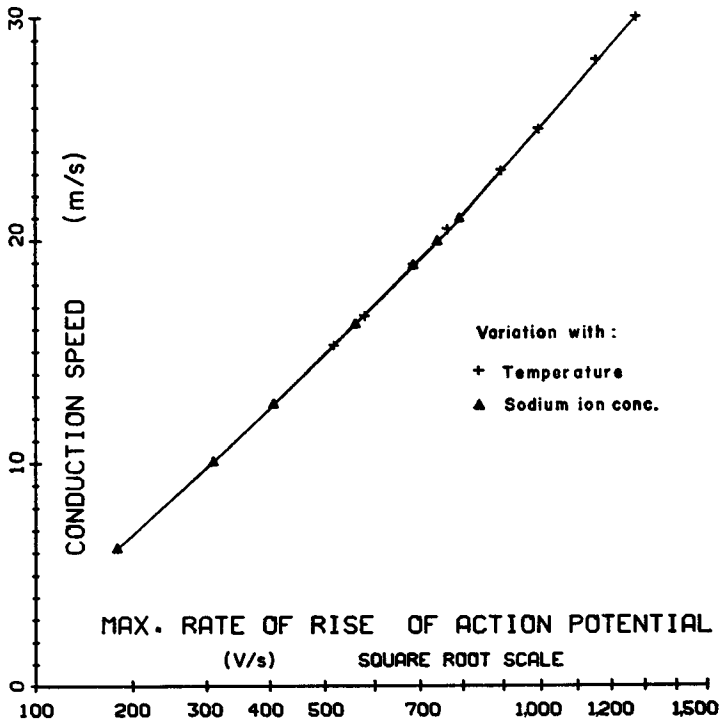

FIGURE 7 The theoretical relationship between conduction speed and maximum rate of rise of an AP in a myelinated nerve cell as they both vary with temperature (+) and with $[Na^+]_o$ (▲).

lated variations of θ and rate of rise of the AP with temperature and with $[Na^+]_o$ changes. While his prediction is not precisely confirmed, the departure from an exact square root dependence is remarkably small. Fig. 7 shows that the square root relation describes the results almost perfectly.

DISCUSSION

The calculations have shown that the mathematical model describes very well the general features of conduction in a myelinated nerve. The match between the shape of the wave forms from the theoretical predictions and the experimental data is excellent, even to the extent of showing the double peak of current through the myelin sheath as the rising phase of an AP passes (Fig. 2 *b*) originally found by Huxley and Stämpfli (1949).

The most obvious difference between propagated responses for *R. pipiens* myelinated nerve from my calculations and those for *X. laevis* calculated by Goldman and Albus (1968) is the slower initial repolarization phase of the *Rana* AP and the rapid final repolarization (shown in Fig. 1 *b*). The calculated wave form for *Rana* agrees quite closely to the experimentally observed shape (Huxley and Stämp-

fli, 1949). The shape of the AP is controlled by the temporal variations of the variables m, h, and n. Clearly the prolonged repolarization and rapid final phase are linked to the plateau in the variable m and the rapid return of m to the resting value (Fig. 1 *c*).

There are a number of marked differences between the theoretical currents reported here for the node of a myelinated axon and the results computed by Hodgkin and Huxley for a propagated response in the squid giant axon (1952 *b*). They found that I_{Na} through the squid axon membrane is comparable in magnitude with I_K. For the nodal membrane, however, I_{Na} is much larger than I_K. The total ion current reverses shortly after the peak of the AP in the squid axon. It remains flowing inward through the nodal membrane for a much longer period, reaching zero and reversing only briefly during the final fast repolarization phase. There are also a number of minor differences made evident in a comparison of the squid and frog model results.

While the calculations have shown that the general form of the response to the stimulation is correct, there is at least one clear difference between the theoretical calculation for propagation in a myelinated nerve and the experimental data. The effect of $[Na^+]_0$ on conduction speed does not agree with the theoretical prediction. The AP propagates about 50% faster than expected when $[Na^+]_0$ is one-fourth of normal. There is some related evidence which also points to a discrepancy at low $[Na^+]_0$ for another nerve preparation. Colquhoun and Ritchie (1972) measured the relative conduction speed of the peak of the compound AP of the nonmyelinated rabbit cervical vagus nerve and found it to be a linear function of the logarithm of relative $[Na^+]_0$ (i.e., the same relationship as my calculation gives for a myelinated axon). These authors used the H.H. theoretical model for the squid axon as an approximate model for the nonmyelinated vagus nerve and solved the equations to obtain conduction speed for various $[Na^+]_0$. Their data show that the predicted relative conduction speed departs significantly at low $[Na^+]_0$ from being a linear function of the logarithm of relative $[Na^+]_0$. Thus I estimate from their data (Fig. 1 *b*) that their predicted conduction speed is as much as 40% lower at one-fourth of the normal $[Na^+]_0$ than their experimental curves would indicate. Thus, insofar as one is justified in using the squid model as a model for mammalian unmyelinated nerve, their data and mine indicate a departure in the same direction between theoretical calculations and real data for low $[Na^+]_0$. Both indicate that the real nerve conducts faster at low $[Na^+]_0$ than is predicted. Although it is not unusual to find divergences between theory and experimental results at extreme ranges of ion concentrations, such divergences do require exploration. For instance, Huxley and Stämpfli (1951 *b*) found that in a solution containing 25% of the normal $[Na^+]_0$, the height of the myelinated AP is about 15% larger than is predicted if the nodal membrane acts like an Na^+ electrode.

There are numerous possible reasons for the difference found between θ (theoretical) and θ (experimental).

(*a*) If choline or tetramethylammonium (TMA^+) ions could pass through the early channel just 5% as well as Na^+, this alone would explain about 40% of the maximum difference between my experimental and theoretical results. Dodge (1963) suggested that the early channel might be partially available to choline, but more recently Hille has shown experimentally that choline ions pass through this channel less than 0.7% as well as Na^+ and that TMA^+ ions pass through less than 0.5% as easily (Hille, 1971 *b*).

(*b*) It was assumed in the simulations that $[Na^+]_i$ is not affected by changes in $[Na^+]_0$. While this is a reasonable assumption (as discussed in the previous paper) for the mean axoplasm $[Na^+]$ for short periods of time after changes of $[Na^+]_0$, it may not be valid for longer periods, and of most importance, it is possible that it is an invalid assumption for $[Na^+]$ in a critical subnodal membrane space. Bergman (1970) has reported voltage clamp evidence for a temporary accumulation of Na^+ near the inner surface of the nodal membrane when the nerve is subjected to a prolonged conditioning volley. He points out that the existence of such a space in which Na^+ ions are collected or at least delayed in diffusion into the bulk of the axoplasm would be quite beneficial for the efficiency of the Na^+ pump system. However, there is no morphological evidence for the existence of such a space.

TABLE II

EFFECT OF CHANGES IN $\Delta\alpha$ ON CONDUCTION SPEED IN NORMAL $[Na^+]$

$\Delta\alpha$	Conduction speed 15°C, $[Na^+]_0$ = 110 mM/liter
	m/s
$\frac{6}{1+\left(\frac{E+25}{18}\right)^2}$ (standard)	18.90
$\frac{6}{1+\left(\frac{E+10}{18}\right)^2}$	15.20
$\frac{6}{1+\left(\frac{E+35}{18}\right)^2}$	23.58
$\frac{8}{1+\left(\frac{E+10}{18}\right)^2}$	16.89
$\frac{8}{1+\left(\frac{E+35}{18}\right)^2}$	32.89

(*c*) The search for the possible causes of the slower than expected conduction speeds with the standard data set of constants (Table I) has provided considerable insight into the sensitivity of conduction speed to the various numerical parameters (Hardy, 1969). A small variation of one parameter has an unexpectedly large effect on speed. In the empirical equations for the dependence of the rate constants (α's and β's) on membrane potential, Dodge included an extra term, $\Delta\alpha$ in the equation for α_m (Eq. 6) which is not found in the equations used for either the squid giant axon (Hodgkin and Huxley, 1952 *b*) or for the toad myelinated nerve (Frankenhauser and Huxley, 1964). This term is used to describe a small perturbation seen on the experimental curve relating α_m to E_N. Evidence for the existence

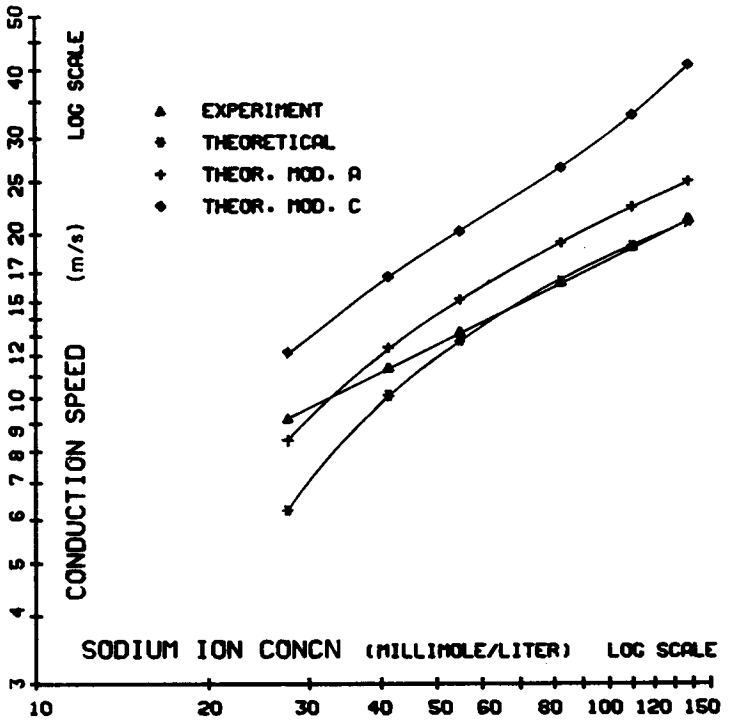

FIGURE 8 The effect on theoretical conduction speed in a myelinated nerve cell as a function of $[Na^+]_0$ resulting from changes in the parameter $\Delta\alpha$.

$$\text{Upper:} \quad \Delta\alpha = 8/\left[1 + \left(\frac{E + 35}{18}\right)^2\right];$$

$$\text{middle:} \quad \Delta\alpha = 8/\left[1 + \left(\frac{E + 25}{18}\right)^2\right];$$

$$\text{lower (standard):} \quad \Delta\alpha = 6/\left[1 + \left(\frac{E + 25}{18}\right)^2\right].$$

The linear curve is the experimental dependence of θ on $[Na^+]_0$.

of such a perturbation for toad myelinated nerve can also be seen in the data of Frankenhauser (1960). The position and height of the bump are quite variable (cf. Dodge, 1963, node 11C and node 12).

In order to determine the effects of changing the height of this bump and its position on the membrane potential axis, Eq. 6 was modified and θ ($[Na^+]_0$ was determined (Fig. 8). Increasing the height of the bump or moving it to the left on the potential axis has the effect of speeding up the rate that m and thus P_{Na} increase with depolarization. Conduction speed in normal $[Na^+]_0$ can be more than doubled by relatively small changes in $\Delta\alpha$ (Table II). The shape of the dependence of θ on $[Na^+]_0$ varies considerably with these alterations and the effects seem to be greater at high $[Na^+]_0$ than at low $[Na^+]_0$. Nevertheless it is clear that a relatively minor variation of $\Delta\alpha$, possibly dependent on $[Na^+]_0$, could be the underlying cause of the discrepancy between the theoretical and experimental dependence of θ on $[Na^+]_0$.

Since there is little if any evidence of a similar perturbation of α_m for the squid giant axon membrane, it would be of interest to determine experimentally how conduction speed varies with $[Na^+]_0$ in that preparation. Of more fundamental interest, however, would be a detailed experimental analysis of $\Delta\alpha$. Does it really exist, and if so, does it depend on $[Na^+]_0$?

I am indebted to Dr. J. Walter Woodbury and Dr. Bertil Hille for support and guidance during the course of this work.

Most of the research is from a Ph.D. thesis and was supported by National Institutes of Health training grants GM-00739 and GM-00260 and by a National Institutes of Health research grant NS-01752 to Dr. Woodbury.
I was also supported by U. S. Public Health Service postdoctoral grant NS-45361.
Computer services were supported by U. S. Public Health Service grant RR-00374 to Dr. T. H. Kehl.

Received for publication 8 October 1972 and in revised form 21 May 1973.

REFERENCES

BENNETT, M. V. L., BERTIL HILLE, and S. OBARA. 1970. *J. Neurophysiol.* **33**:585.
BERGMAN, CLAUDE. 1970. *Pfluegers Arch. Eur. J. Physiol.* **317**:287.
COLQUHOUN, D., and J. M. RITCHIE. 1972. *J. Physiol. (Lond.).* **221**:533.
DODGE, F. A. 1961. *In* Biophysics of Physiological and Pharmacological Actions. American Association for the Advancement of Science, Washington, D. C.
DODGE, F. A. 1963. A study of ionic permeability changes in myelinated nerve fibres of the frog. Ph.D. Thesis: The Rockefeller Institute, New York. University Microfilms, Inc., Ann Arbor, Mich. (no. 64-7333).
FITZHUGH, R. 1962. *Biophys. J.* **2**:11.
FRANKENHAEUSER, B. 1960. *J. Physiol. (Lond.).* **151**:491.
FRANKENHAEUSER, B., and A. F. HUXLEY. 1964. *J. Physiol. (Lond.).* **171**:302.
FRANKENHAEUSER, B., and L. E. MOORE. 1963. *J. Physiol. (Lond.).* **169**:431.
GOLDMAN, L., and J. S. ALBUS. 1968. *Biophys. J.* **8**:596.
HARDY, W. L. 1969. Propagation in myelinated nerve: dependence on external sodium. Ph.D. Thesis. The University of Washington, Seattle, Wash. University Microfilms Inc., Ann Arbor, Mich. (no. 70-14,762.

HARDY, W. L. 1971. *Biophys. Soc. Annu. Meet. Abstr.* **11**:238a.
HARDY, W. L. 1973. *Biophys. J.* **13**:1054.
HARDY, W. L., and J. W. WOODBURY. 1970. *Biophys. Soc. Annu. Meet. Abstr.* **10**:112a.
HILLE, B. 1967. A pharmacological analysis of the ionic channels of nerve. Ph.D. Thesis. The Rockefeller University, New York. University Microfilms Inc., Ann Arbor, Mich. (no. 68-9584).
HILLE, B. 1970. *Prog. Biophys. Mol. Biol.* **21**:1.
HILLE, B. 1971 *a. In* Biophysics and Physiology of Excitable Membranes. W. J. Adelman, Jr., editor. Van Nostrand Reinhold Company, New York.
HILLE, B. 1971 *b. J. Physiol. (Lond.).* **58**:599.
HODGKIN, A. L. 1964. The Conduction of the Nervous Impulse. Charles C Thomas, Publisher, Springfield, Ill.
HODGKIN, A. L., and A. F. HUXLEY. 1952 *a. J. Physiol. (Lond.).* **116**:497.
HODGKIN, A. L., and A. F. HUXLEY. 1952 *b. J. Physiol. (Lond.).* **117**:500.
HODGKIN, A. L., and B. KATZ. 1949. *J. Physiol. (Lond.).* **108**:37.
HUTCHINSON, N. A., Z. J. KOLES, and R. S. SMITH. 1970. *J. Physiol. (Lond.).* **208**:279.
HUXLEY, A. F., and R. STÄMPFLI. 1949. *J. Physiol. (Lond.).* **108**:315.
HUXLEY, A. F., and R. STÄMPFLI. 1951*a. J. Physiol. (Lond.).* **112**:476.
HUXLEY, A. F., and R. STÄMPFLI. 1951 *b. J. Physiol. (Lond.).* **112**:496.
KELLEY, L. G. 1967. Handbook of Numerical Methods and Applications. Addison-Wesley Publishing Co., Inc., Reading, Mass.
SMITH, R. S., and Z. J. KOLES. 1970. *Am. J. Physiol.* **219**:1256.
TASAKI, I. 1955. *Am. J. Physiol.* **181**:639.
TAYLOR, R. E., and W. K. CHANDLER. 1962. *Biophys. Soc. Annu. Meet. Abstr.* TD1.